MJFAS MALAYSIAN JOURNAL OF FUNDAMENTAL AND APPLIED SCIENCES
PRINT ISSN: 2289-5981 | ONLINE ISSN: 2289-599X

RESEARCH ARTICLE

Investigation of active species in methanation reaction over cerium based loading

Salmiah Jamal Mat Rosid [a, *], Wan Azelee Wan Abu Bakar [b], Susilawati Toemen [b], Nurulhuda Mohamad Yusoff [a], Azman Azid [c], Wan Nur Aini Wan Mokhtar [d]

[a] *UniSZa Science and Medicine Foundation Centre, Universiti Sultan Zainal Abidin, Kampus Gong Badak, 21300 Kuala Nerus, Terengganu, Malaysia*
[b] *Department of Chemistry, Faculty of Science, Universiti Teknologi Malaysia, 81310 UTM Johor Bahru, Johor, Malaysia*
[c] *Faculty of Bioresources and Food Industry, Universiti Sultan Zainal Abidin, Besut Campus, 22200 Besut, Terengganu, Malaysia*
[d] *Faculty of Science and Technology, Universiti Kebangsaan Malaysia, 43600 Bangi, Selangor, Malaysia*

* *Corresponding author: salmiahjamal@unisza.edu.my*

Article history
Received 28 December 2018
Revised 22 February 2019
Accepted 4 April 2019
Published Online 15 May 2019

Graphical abstract

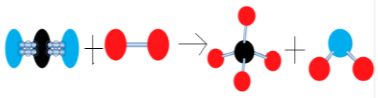

$CO_2 + H_2 \rightarrow CH_4 + H_2O$

Abstract

A series of cerium oxide based catalyst has been studied by various cerium loadings that calcined at 1000°C using wet impregnation method. The potential Ru/Mn/Ce (5:35:60) /Al_2O_3 catalyst calcined at 1000°C was characterized using XRD, XPS, and BET analyses. As could be observed from the XRD analysis, at Ce ratio of 55% and 65%, both revealed the presence of RuO_2 with tetragonal phase and intense, sharper peaks indicating to high crystallinity and in line with lower surface area, 50.95 m^2/g in BET analysis. Meanwhile, CeO_2 (cubic phase) and MnO_2 (tetragonal phase) were also observed for 55%, 60%, and 65%, respectively. However, the presence of Al_2O_3 with rhombohedral phase at 55% and 65% was revealed as an inhibitor which decreased the CO_2 conversion. The presence of active species on Ru/Mn/Ce (5:35:60) /Al_2O_3 catalyst has been confirmed using XPS analysis with the deconvolution peaks belonged to Ce^{4+} with the formation of CeO_2 compound and Mn^{4+} for MnO_2. The product formed in catalytic methanation was proposed to be H_2O and CH_3OH from GC and HPLC analysis.

Keywords**:** Cerium, catalyst, carbon dioxide, methanation

INTRODUCTION

In Malaysia, urban dwellers have rapidly increased and at the same time, claims for certain types of products have been increased to meet the demands of the present society. Modern societies are relied heavily on vehicles like cars, trucks and trains. The release of the vehicle is depended primarily on the burning of fossil fuels, thereby contributing to the dominant greenhouse gases (CO_2, SO_2, NO_2) emitted in the air either inside or around the world. Carbon dioxide is the most important greenhouse gas generated by transport activities and it affects the global warming if its emission is not been controlled or reduced, as investigated by Yusof *et al*. (2010). Carbon dioxide must be eliminated to prevent or reduce harmful gases that released to the environment. This will reduce problem such as acid rain, ozone reduction, or greenhouse gases. Therefore, appropriate methods are needed to overcome this problem. Recently, alternative methods have been developed, such as the conversion of CO_2 catalysts through the methanation reaction. The catalytic methanation reaction refers to the process of converting carbon monoxide and carbon dioxide from the gas stream to produce methane using catalyst (Mills and Fred, 1974). This will eliminate toxic carbon dioxide and produce methane at the same time. It is also economically viable because the catalyst is recyclable and ecologically correct, as it does not release toxic gases into the air during the reaction. As the catalytic methanation reaction has been proven to provide an excellent performance of converting CO_2 in the simulated natural gas in the previous study using Ru/Mn/Ce-Al_2O_3 (Rosid *et al.*, 2018a), therefore, the present study was steered in order to study the effect of based cerium, ruthenium and catalyst loading using double reactor towards catalytic activity and physicochemical properties at low reaction temperature.

EXPERIMENTAL

Materials

Chemicals used in this research were cerium(III) nitrate hexahydrate (Sigma Aldrich Chemical), ruthenium(III) chloride (Molekula), aluminium oxide (MERCK Eurolab), and manganese nitrate tetrahydrate (Sigma Aldrich Chemical).

Synthesis of Ru/Mn/Ce catalyst

Cerium salt was weighed (5g) in a beaker together with manganese and ruthenium according to the desired ratio and they were dissolved in small amount of distilled water. Then, the solutions were mixed together and stirred continuously by magnetic bar for 30 minutes at room temperature to homogenize the mixture. Then, alumina beads with diameter of 3 mm were immersed into the catalysts solution for 20 minutes and the supported catalysts were transferred onto evaporating dish with glass wool on it. They were then aged in an oven at 80–90°C for 24 hours to remove water and allow good coating of the metal on the surface of the supported catalysts. They were then calcined in the furnace at 400°C for 5 hours under ambient atmosphere using a ramp rate of 10°C/min to eliminate all the impurities, metal precursors and excess of water. The steps were repeated and applied for all different ratios of catalysts.

Catalytic activity using FTIR, GC, and HPLC

The reaction gas mixture consisting of CO_2 and H_2 in a 1:4 molar ratio was continuously passed through the catalyst and heated in an isothermal tubular furnace. The product stream was collected on a FTIR sample cell with attached KBr windows and scanned using the Nicolet Avatar 370 DTGS FTIR spectrophotometer. Gaseous products were periodically analyzed by gas chromatography to determine the formation of methane from CO_2 conversion reaction. The Hewlett Packard 6890 Series gas chromatography system via flame ionization detector (FID) was set at initial temperature of 40ºC for 7 minutes and at injection temperature of 150ºC. The presence of methanol content was observed by HPLC (Rezex ROA- organic acid) using a column of 300 mm×7.8 mm ID with Refractive Index (RI) detector with 0.005 N sulfuric acid as an eluent.

Characterization

In XRD analysis, the sample was manually crushed into fine powder and then placed into the sample holder. The XRD pattern was recorded by the D5000 Siemens Crystalloflex Diffractometer with Cu Kα radiation (λ=1.54060 Å). The spectrometer of XPS was flushed by using argon gas at 6×10^{-9} Torr before putting the sample for spectrum recording to maintain sample surface integrity. Before analyzing the sample, the spectrometer was calibrated using a clean argentum crucible by assuming that the binding energy for Ag 3 *d*5/2 was 368.25 eV. From the spectrum, the peak for C 1*s* was obtained at binding energy of 284.5 eV, which could be taken as the second reference. Dried powder sample was analyzed by Kratos surface analysis spectrometer XSAM HS instrument using MgKα (1253.6 eV) as the X-ray source.

RESULTS AND DISCUSSION

Characterization of catalyst

Different Ce loadings revealed almost similar diffractograms, as shown in Fig. 1, where the peak was more intense and sharper, with high crystallinity. As could be observed, at ratio of 55% and 65%, both showed the existence of RuO_2 species with tetragonal phase. The phases detected at 55% of Ce loading were CeO_2 (cubic), Al_2O_3 (cubic), MnO_2 (tetragonal), Al_2O_3 (rhombohedral) and RuO_2 (tetragonal). CeO_2 with cubic phase was revealed at 2θ values of 28.48° (I_{100}), 47.43° (I_{45}), 56.40° (I_{33}), 33.33° (I_{27}), 76.20° (I_{10}) and 79.04° (I_6). Meanwhile, cubic Al_2O_3 was detected at 2θ values of 67.17° (I_{100}), 45.43° (I_{100}), 36.82° (I_{90}) and 60.45° (I_{70}). The overlapping peaks of MnO_2 with tetragonal phase were observed at 2θ value of 28.48° (I_{100}), 36.87° (I_{52}), 56.54° (I_{48}), and 70.09° (I_{30}). According to Wang *et al.* (2016), the structural characterization on unsupported and supported MnO_x catalysts preferred MnO_2 as an active species. Other than that, the peak of RuO_2 (tetragonal) was observed to be appeared at 2θ values of 35.50° (I_{77}), 44.12° (I_{50}), and 54.86° (I_{45}). Interestingly, new peaks that assigned to corundum rhombohedral Al_2O_3 were detected at 2θ values of 35.122° (I_{100}), 43.317° (I_{96}), 57.469° (I_{91}), 25.583° (I_{68}), and 52.534 (I_{47}). As reported by Matori *et al.* (2012), the rhombohedral of Al_2O_3 was appeared at calcination temperature above 880ºC. The rhombohedral α-Al_2O_3 is the stable phase through the nucleation and the crystallite growth process. Therefore, it was capable in increasing the particle size which then causing in a decrease of the surface area. In consequence, it would lower the catalytic activity. Similar observation was also detected for the catalyst that calcined at 1000°C for ratio of 65%. However, in the diffractogram for ratio of 60%, only Al_2O_3 cubic, CeO_2 cubic and MnO_2 tetragonal phase were detected. The Al_2O_3 cubic was revealed at 2θ values of 67.13° (I_{100}), 45.60° (I_{100}), and 36.46° (I_{90}), while the peak for cerium oxide cubic has been assigned at 2θ values of 28.51° (I_{100}), 47.41° (I_{45}), 56.43° (I_{33}), 33.13° (I_{27}), 76.36° (I_{10}) and 79.02° (I_6). Meanwhile, MnO_2 with tetragonal phase was observed at 2θ values of 28.56° (I_{100}), 36.98° (I_{52}) and 56.60° (I_{48}).

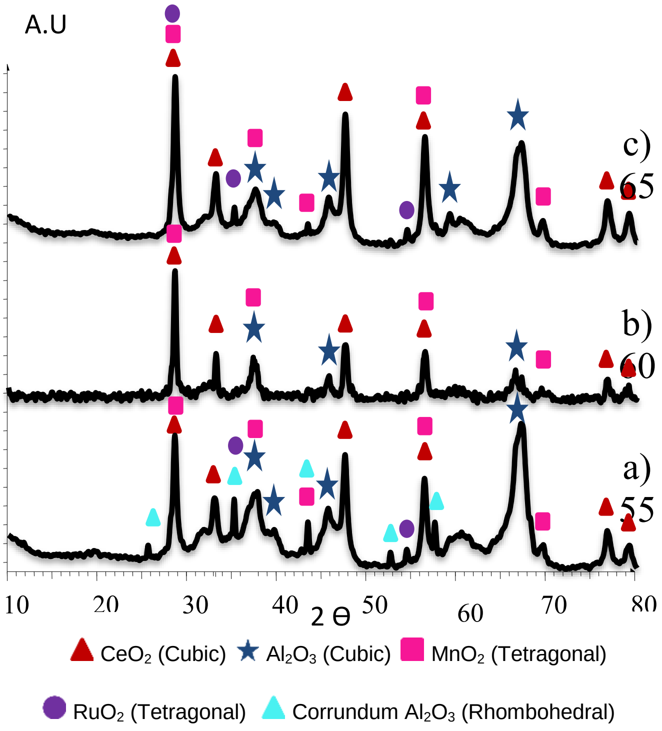

Fig. 1 XRD diffraction patterns of Ru/Mn/Ce-Al_2O_3 catalyst calcined at 1000ºC for 5 hours with various based loadings, a) 55%, b) 60% and c) 65%.

XPS was used to determine the composition of the elements in the catalyst and the chemical state of the element. In this study, the charge of the specimen, the C 1*s* line (284.50 eV) was used as the standard. The peak of Ru was not detected in Ru/Mn/Ce (5:35:60)/Al_2O_3 and this result was supported with XRD, in which no peak of Ru was observed. Fig. 2 displays the wide scan of the XPS spectrum based on the existence of different types of elements in the Ru/Mn/Ce (5:35:60)/Al_2O_3 catalyst sample calcined at 1000ºC.

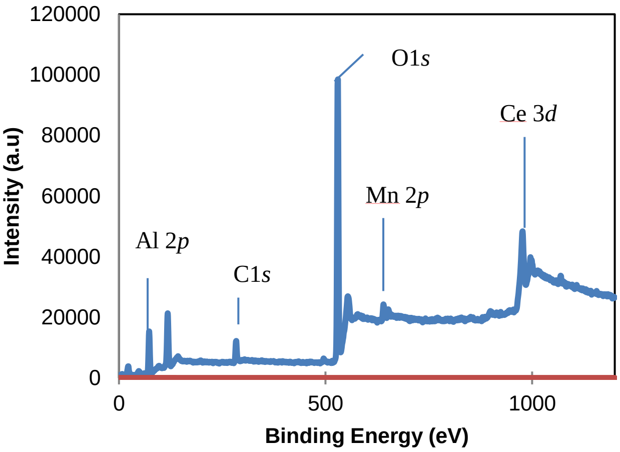

Fig. 2 Wide scan of XPS spectrum obtained from fresh Ru/Mn/Ce (5:35:60)/Al_2O_3 catalyst calcined at 1000ºC for 5 hours.

The atomic concentration of Ce detected by XPS was low (<0.20%), indicating the partial surface encapsulation of Ce and slow formation of oxygen vacancy on the alumina support, as also observed by Luches and Valeri (2015). According to XPS NIST database, the deconvolation peaks were belonged to Ce^{4+} with the formation of CeO_2 compound, as shown in Fig. 3. Typically, Ce 3*d* XPS core-level spectra exhibited three-lobed envelopes (around 879–890 eV, 895–910 eV and approximately 916 eV). The peak of cerium was decomposed into six components to form two doublets. The first doublet was corresponded to Ce 3$d_{5/2}$ (*E*b = 882.16 ev) and Ce 3$d_{5/2}$ (*E*b = 887.09 ev). The second doublet was corresponded to Ce 3$d_{3/2}$ (*E*b = 900.89 ev) and Ce 3$d_{3/2}$ (*E*b = 904.15 ev), while the third doublet at Ce 3$d_{3/2}$ (*E*b = 907.50 ev) and Ce 3$d_{5/2}$ (*E*b = 884.41 ev) were attributed to cerium under its oxidized form. As could be seen, there was no systematic evolution in the positions of different peaks in which suggesting that the presence of manganese oxides did not alter the cerium chemical environments as it formed a synergistic interaction between manganese and ceria species as discussed by Liu *et al.* (2015). This finding was supported with XRD data where CeO_2 was observed in the diffractogram (Fig. 1).

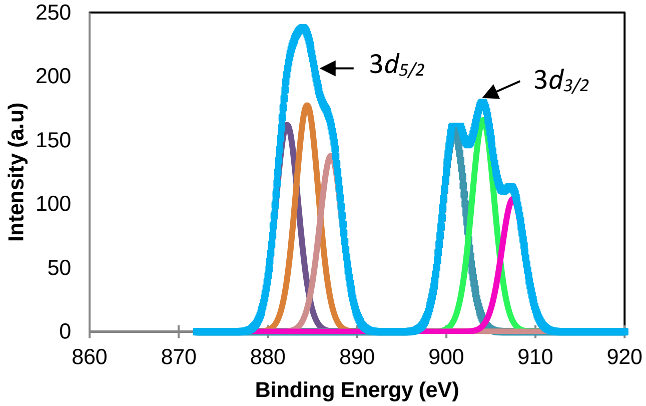

Fig. 3 High resolution Ce 3*d* XPS spectra obtained from fresh Ru/Mn/Ce (5:35:60)/Al_2O_3 catalyst calcined at 1000°C for 5 hours.

XPS spectra for Mn 2*p* were consisted of two doublets as shown in Fig. 4, which were Mn 2$p_{1/2}$ and 2$p_{3/2}$. According to literature, the binding energy, *E*b of Mn 2$p_{3/2}$ in pure manganese oxides could be found at 641.2 eV (Mn^{2+}), 641.8 eV (Mn^{3+}), and 642.1 eV (Mn^{4+}), respectively. In this study, a compound with MnO_2 (Mn^{4+}) was observed at peak E_b value of 642.26 eV. This was in a good agreement with XRD analysis which MnO_2 species was observed in the diffractogram. Deconvulation of Mn 2p produced 2 peaks at E_b value of 642.26 eV and 644.49 eV for Mn 2$p_{3/2}$, which were attributed to MnO_2 species. Meanwhile for Mn 2$p_{1/2}$, 2 peaks at E_b value of 654.36 eV and 656.32 eV were also attributed to MnO_2. The other two peaks with binding energy at E_b value of 641.82 eV and 653.05 eV were assigned to Mn_2O_3 species. However, this species was not observed in XRD analysis, which suggested that this was not an active species.

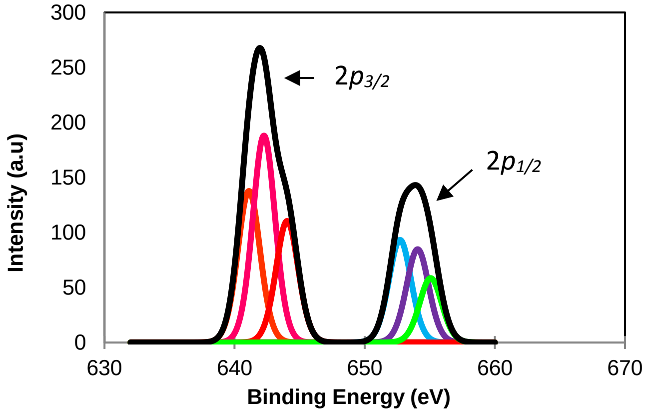

Fig. 4 High resolution Mn 2*p* XPS spectra obtained from fresh Ru/Mn/Ce (5:35:60)/Al_2O_3 catalyst calcined at 1000°C for 5 hours.

The BET analysis showed that when cerium loading was increased to 65%, the surface area was decreased from 50.95 m^2/g to 32.72 m^2/g due to the removal of pores and the formation of dense solid as been discussed by Rosid *et al*. (2018). Therefore, it could be concluded that high surface area was important in catalytic activity since it would provide more active surfaces for catalytic interaction. The BJH pore size distribution indicated a pore diameter of around 75-120 nm and this was supported with smaller hysteresis. The presence of a single peak from the graph of pore size distribution in Fig. 5 was indicated to the presence of pores in the catalyst sample. The plot was corresponded to the Type IV isotherm and H3 hysteresis which consisted of aggregated or agglomerated particle in forming non-uniform slit shaped pores for the adsorption of CO_2 and H_2 gases as investigated by Thommes *et al*. (2015).

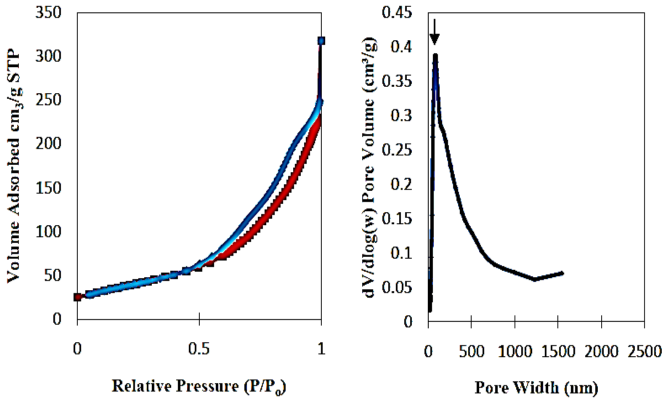

Fig. 5 Isotherm plot and pore size distribution of nitrogen adsorption for Ru/Mn/Ce (5:35:60)/Al_2O_3 catalyst calcined at 1000°C for 5 hours.

Catalytic activity of cerium oxide

Effect of various metal oxide based loadings

The potential catalyst, Ru/Mn/Ce-Al_2O_3 was optimized using different cerium based loadings to observe its effect on the catalytic activity. The ratios of 50-85 wt% of cerium oxide catalysts were selected. Fig. 6 showed that the trend plots of catalytic performance when the Ce content was increased to 60%, the conversion of CO_2 was increased, but it was decreased as the Ce content was up to 85%. Perhaps, this was due to the blocking of surface active sites and pore structure by excessive loading of Ce, promoting the particle to nucleate as well as inhibiting the growth of crystal (Rosid *et al.*, 2019). Therefore, the optimum cerium loading was 60%, which gave 100% CO_2 conversion.

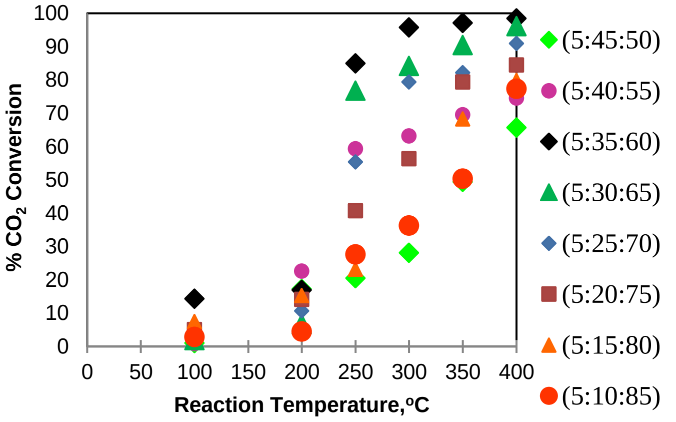

Fig. 6 CO_2 conversion of Ru/Mn/Ce/Al_2O_3 catalyst calcined at 1000°C for 5 hours with different cerium based loadings.

Effect of various ruthenium loadings

The catalytic activities of potential catalyst with different ruthenium loadings (5 wt%, 10 wt%, and 15 wt%) were investigated. CO_2 conversion for each catalyst was started to increase significantly at 250°C reaction temperature. Fig. 7 showed that the CO_2 conversion was decreased as the ruthenium loading was increased. As a result, the optimum ruthenium loadings to achieve higher CO_2 conversion was 5 wt%. This behavior might be due to an excessive distribution of ruthenium content on the support surface as suggested by Zhang *et al.* (2012). This finding was also in an agreement with a study conducted by Rosid *et al.*, (2015), which stated that the addition of 5 wt% of ruthenium to lanthanum oxide catalyst could enhance the catalytic activity by achieving almost 100% of CO_2 conversion.

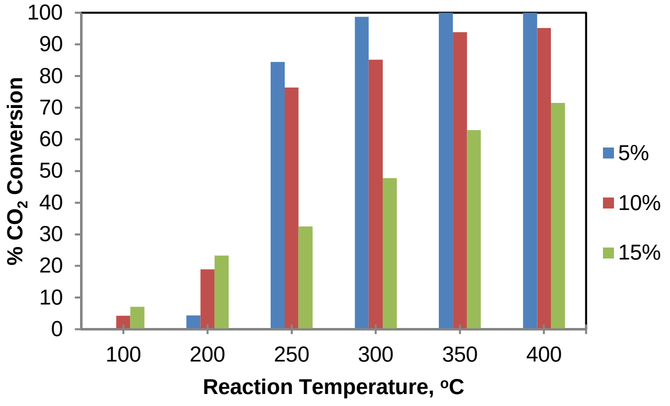

Fig. 7 CO_2 conversion of $Ru/Mn/Ce/Al_2O_3$ catalyst calcined at 1000°C for 5 hours with different ruthenium loadings.

Catalyst testing on CO_2 methanation reaction using double reactors

In this section, the $Ru/Mn/Ce(5:35:60)/Al_2O_3$ catalyst was tested using two reactors instead of using one reactor, as in previous section. This testing was conducted using two isothemal furnaces connected in series. The catalyst loading was doubled in this process to examine the conversion percentage when more catalysts were utilized. Using two reactors in the catalytic activity process was also relevant in providing more time for the reaction to occur in order to maximize conversion of CO_2. This method was also suitable for industrial application. Fig. 8 showed that the percentage of CO_2 conversion over $Ru/Mn/Ce(5:35:60)/Al_2O_3$ catalyst calcined at 1000°C by double reactor was 95.83% at 350°C reaction temperature. The performance of the catalyst was slightly lower compared to single reactor over the same catalyst that achieved 100% at the same reaction temperature. The findings by Li *et al.*, (2014) were in agreement with our results that stated the decrease of CO_2 conversion in the second reactor might be caused by the formation of water in the first reactor at low temperature which blocked the catalyst surface during reaction at the first reactor.

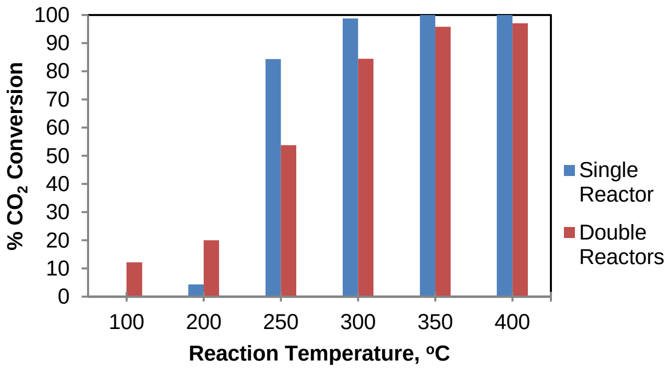

Fig. 8 CO_2 conversion of $Ru/Mn/Ce(5:35:60)/Al_2O_3$ catalyst calcined at 1000°C for 5 hours with double reactor.

Methane formation by gas chromatography

The $Ru/Mn/Ce\text{-}Al_2O_3$ catalyst was further investigated to determine the production of methane by GC analysis. The results showed that no methane product was formed at initial reaction temperatures of 100°C and 200°C. As the reaction temperatures were raised up to 300°C, 350°C, and 400°C, about 40.71%, 66.80% and 78.00% of methane were formed respectively at 1000°C of calcination temperature. Meanwhile, for $Ru/Mn/Ce$ (5:40:55)/Al_2O_3 and $Ru/Mn/Ce$ (5:30:65)/Al_2O_3, the methane products that formed were 35.54% and 42.87%, respectively at 400°C of reaction temperature. The results showed that $Ru/Mn/Ce$ (5:35:60)/Al_2O_3 calcined at 1000°C was assigned as the potential catalyst among other studied cerium catalysts due to high methane formation. High methane formation achieved at high reaction temperatures might be due to high exothermic reactions where the methane reaction was favored at high temperatures.

Detection of methanol by high performance liquid chromatography (HPLC)

The methane formation which detected by GC using a single reactor for this potential catalyst was far from the value of CO_2 conversion. Therefore, HPLC tests were conducted to confirm the presence of methanol as a side product. The HPLC analysis illustrated that the compound of interest was eluted at retention time of 20 min for standard methanol. When the sample was injected, peaks were started to appear at 20 min of retention and assigned to methanol compound as it was compatible with standard methanol (not shown).

CONCLUSION

The potential $Ru/Mn/Ce(5:35:60)\text{-}Al_2O_3$ catalysts with various based cerium, ruthenium, and catalyst loadings have shown an effect towards catalytic activity and physicochemical properties. The percentages of CO_2 conversion for $Ru/Mn/Ce(5:40:55)\text{-}Al_2O_3$, $Ru/Mn/Ce(5:35:60)\text{-}Al_2O_3$, and $Ru/Mn/Ce(5:30:65)\text{-}Al_2O_3$ were 74.53%, 100% and 96.12%, respectively at 400°C of reaction temperature. The products of this reaction were confirmed to be H_2O, CH_4 and CH_3OH. The XRD analysis revealed that the active species in the potential catalyst were CeO_2 and MnO_2, meanwhile corruncum rhombohedral Al_2O_3 was assigned as an inhibitor species at 55% and 65% cerium loading. The presence of active species was supported with XPS analysis and BET analysis showed that the surface area was lower for 55% and 65% with 27.23 m^2/g and 32.72 m^2/g, respectively.

ACKNOWLEDGEMENT

The authors would like to thank to Universiti Sultan Zainal Abidin, Universiti Teknologi Malaysia and Ministry of Higher Education (MOHE), Malaysia for financial support.

REFERENCES

Li C. Yuan X. and Fujimoto K. 2014. Development of highly stable catalyst for methanol synthesis from carbon dioxide. *Applied Catalysis A: General* 469, 306-311.

Liu L. Shi J. Zhang X. Liu J. Z. 2015. Flower like Mn-doped CeO_2 microstructure: Synthesis, characterization and catalytic properties. *Journal of Chemistry*, Article ID 254750. 1-11.

Luches P. and Valeri S. 2015. Structure, morphology and reducibility of epitaxial cerium oxide ultrathin films and nanostructures. *Materials (Basel)* 8(9), 5818-5833.

Matori K. A. Wah L. C. Hashim M. Ismail I. and Zaid M. H. M. 2012. Phase transformation of alumina made from waste aluminium via a precipitation technique. *International Journal of Molecular Science* 13(12), 16812-16821.

Mills G. A. and Fred W. S. 1974. Catalytic methanation. *Catalysis Review: Science and Engineering* 8(1), 159-210.

Rosid, S. J. M, Bakar, W. A. W. A. and Ali, R. 2015. Physicochemical study of supported cobalt-lanthanum oxide based catalysts for CO_2/H_2 methanation reaction. *Clean Technology Environmental Policy*, 17(1), 257-264.

Rosid, S. J. M, Bakar, W. A. W. A. and Ali, R. 2018. Characterization and modelling optimization on methanation activity using Box-Behnken design through cerium doped catalysts. *Journal of Cleaner Production*. 170. 278-287.

Rosid, S. J. M., Toemen, S., Bakar, W. A. W. A., Zamani, A. H., and Mokhtar W. N. A. W. 2019. Physicochemical characteristic of neodymium oxide-based catalyst for in-situ CO_2/H_2 methanation reaction. *Journal of Saudi Chemical Society*. 23, 284-293.

Thommes, M., Kaneko, K., Neimark, A. V., Oliver, J. P., Rodrigue-Reinoso, F., Ronquerol, J., and Sing, K. S. W. 2015. Physisorption of gases, with special reference to the evaluation of surface area and pore size distribution (IUPAC Technical Report). *Pure and Applied Chemistry* 87(9-10). 1051-1069.

Wang, L., He, H., Zhang, C., Wang, Y., and Zhang, B. 2016. Effect of precursors for manganese loaded γ-Al_2O_3 catlaysts on plasma-catalytic removal of o-xylene. *Chemical Engineering Journal* 288(C), 406-413.

Yusof, N. B. M., Mohamad, F. I, Ruslan, H. 2010. Estimation of dispersion of carbon monoxide (CO), nitrogen dioxide (NO_2), and carbon dioxide (CO_2) from Port Klang - KLIA Road. Universiti Teknologi Nasional, Malaysia.

Zhang, Y. F., Zhang, G., Wang, L., Xu, Y., Sun, Y. 2012. Selective methanation of carbon monoxide over Ru based catalysts in H_2-rich gases. *Journal of Industrial and Engineering Chemistry* 18(5), 1590-1597.